One-dimensional parabolic-beam photonic crystal laser

Byeong-Hyeon Ahn,[1,5,6] Ju-Hyung Kang,[1,5,7] Myung-Ki Kim,[1,2] Jung-Hwan Song,[1] Bumki Min,[2] Ki-Soo Kim,[3] and Yong-Hee Lee[1, 4]

[1]*Department of Physics, Korea Advanced Institute of Science and Technology, Daejeon 305-701, Korea*
[2]*Department of Mechanical Engineering, Korea Advanced Institute of Science and Technology, Daejeon 305-701, Korea*
[3]*Convergence and Components & Materials Research Laboratory, Electronics and Telecommunications Research Institute, Daejeon 305-700, Korea*
[4]*Department of Physics and Department of Nanoscience and Technology (WCU), Korea Advanced Institute of Science and Technology, Daejeon 305-701, Korea*
[5]*These authors contributed equally to this work.*
[6]*seygene@kaist.ac.kr*
[7]*kangjuhy@kaist.ac.kr*

Abstract: We report one-dimensional (1-D) parabolic-beam photonic crystal (PhC) lasers in which the width of the PhC slab waveguide is parabolically tapered. A few high-Q resonant modes are confirmed in the vicinity of the tapered region where Gaussian-shaped photonic well is formed. These resonant modes originate from the dielectric PhC guided mode and overlap with the gain medium efficiently. It is also shown that the far-field radiation profile is closely associated with the symmetry of the structural perturbation.

OCIS codes: (203.5298) Photonic crystals; (140.3945) Microcavities; (250.5300) Photonic integrated circuits; (140.5960) Semiconductor lasers.

References and links

1. O. Painter, R. K. Lee, A. Scherer, A. Yariv, J. D. O'Brien, P. D. Dapkus, and I. Kim I, "Two-dimensional photonic band-Gap defect mode laser," Science **284**(5421), 1819–1821 (1999).
2. H.-G. Park, S.-H. Kim, S.-H. Kwon, Y.-G. Ju, J.-K. Yang, J.-H. Baek, S.-B. Kim, and Y.-H. Lee, "Electrically driven single-cell photonic crystal laser," Science **305**(5689), 1444–1447 (2004).
3. M.-K. Seo, K.-Y. Jeong, J.-K. Yang, Y.-H. Lee, H.-G. Park, and S.-B. Kim, "Low threshold current single-cell hexapole mode photonic crystal laser," Appl. Phys. Lett. **90**(17), 171122 (2007).
4. H. Altug, D. Englund, and J. Vŭcković, "Ultrafast photonic crystal nanocavity laser," Nat. Phys. **2**(7), 484–488 (2006).
5. T. Baba, D. Sano, K. Nozaki, K. Inoshita, Y. Kuroki, and F. Koyama, "Observation of fast spontaneous emission decay in GaInAsP photonic crystal point defect nanocavity at room temperature," Appl. Phys. Lett. **85**(18), 3989–3991 (2004).
6. T. Tanabe, M. Notomi, S. Mitsugi, A. Shinya, and E. Kuramochi, "All-optical switches on a silicon chip realized using photonic crystal nanocavities," Appl. Phys. Lett. **87**(15), 151112 (2005).
7. M.-K. Kim, I.-K. Hwang, S.-H. Kim, H.-J. Chang, and Y.-H. Lee, "All-optical bistable switching in curved microfiber-coupled photonic crystal resonators," Appl. Phys. Lett. **90**(16), 161118 (2007).
8. A. J. Shields, "Semiconductor quantum light sources," Nat. Photonics **1**(4), 215–223 (2007).
9. W.-H. Chang, W.-Y. Chen, H.-S. Chang, T.-P. Hsieh, J.-I. Chyi, and T.-M. Hsu, "Efficient single-photon sources based on low-density quantum dots in photonic-crystal nanocavities," Phys. Rev. Lett. **96**(11), 117401 (2006).
10. C. Santori, D. Fattal, J. Vucković, G. S. Solomon, and Y. Yamamoto, "Indistinguishable photons from a single-photon device," Nature **419**(6907), 594–597 (2002).
11. T. Yoshie, A. Scherer, J. Hendrickson, G. Khitrova, H. M. Gibbs, G. Rupper, C. Ell, O. B. Shchekin, and D. G. Deppe, "Vacuum Rabi splitting with a single quantum dot in a photonic crystal nanocavity," Nature **432**(7014), 200–203 (2004).
12. K. Hennessy, A. Badolato, M. Winger, D. Gerace, M. Atatüre, S. Gulde, S. Fält, E. L. Hu, and A. Imamoğlu, "Quantum nature of a strongly coupled single quantum dot-cavity system," Nature **445**(7130), 896–899 (2007).
13. D. Englund, A. Faraon, I. Fushman, N. Stoltz, P. Petroff, and J. Vucković, "Controlling cavity reflectivity with a single quantum dot," Nature **450**(7171), 857–861 (2007).
14. H. Mabuchi, and A. C. Doherty, "Cavity quantum electrodynamics: coherence in context," Science **298**(5597), 1372–1377 (2002).
15. G. Khitrova, H. M. Gibbs, M. Kira, S. W. Koch, and A. Scherer, "Vacuum Rabi splitting in semiconductors," Nat. Phys. **2**(2), 81–90 (2006).

#122441 - $15.00 USD Received 8 Jan 2010; revised 25 Feb 2010; accepted 1 Mar 2010; published 4 Mar 2010

16. B. S. Song, S. Noda, T. Asano, and Y. Akahane, "Ultra-high-Q photonic double-heterostructure nanocavity," Nat. Mater. **4**(3), 207–210 (2005).
17. T. Tanabe, M. Notomi, E. Kuramochi, A. Shinya, and H. Taniyama, "Trapping and delaying photons for one nanosecond in an ultrasmall high-Q photonic-crystal nanocavity," Nat. Photonics **1**(1), 49–52 (2007).
18. B. Schmidt, Q. Xu, J. Shakya, S. Manipatruni, and M. Lipson, "Compact electro-optic modulator on silicon-on-insulator substrates using cavities with ultra-small modal volumes," Opt. Express **15**(6), 3140–3148 (2007).
19. M. Notomi, E. Kuramochi, and H. Taniyama, "Ultrahigh-Q nanocavity with 1D photonic gap," Opt. Express **16**(15), 11095–11102 (2008).
20. M. Eichenfield, R. Camacho, J. Chan, K. J. Vahala, and O. Painter, "A picogram- and nanometre-scale photonic-crystal optomechanical cavity," Nature **459**(7246), 550–555 (2009).
21. J. Chan, M. Eichenfield, R. Camacho, and O. Painter, "Optical and mechanical design of a "zipper" photonic crystal optomechanical cavity," Opt. Express **17**(5), 3802–3817 (2009).
22. P. B. Deotare, M. W. McCutcheon, I. W. Frank, M. Khan, and M. Lončar, "High quality factor photonic crystal nanobeam cavities," Appl. Phys. Lett. **94**(12), 121106 (2009).
23. L.-D. Haret, T. Tanabe, E. Kuramochi, and M. Notomi, "Extremely low power optical bistability in silicon demonstrated using 1D photonic crystal nanocavity," Opt. Express **17**(23), 21108–21117 (2009).
24. M. W. McCutcheon, and M. Lončar, "Design of a silicon nitride photonic crystal nanocavity with a Quality factor of one million for coupling to a diamond nanocrystal," Opt. Express **16**(23), 19136–19145 (2008).
25. C. Sauvan, G. Lecamp, P. Lalanne, and J. P. Hugonin, "Modal-reflectivity enhancement by geometry tuning in Photonic Crystal microcavities," Opt. Express **13**(1), 245–255 (2005).
26. M.-K. Kim, I.-K. Hwang, M.-K. Seo, and Y.-H. Lee, "Reconfigurable microfiber-coupled photonic crystal resonator," Opt. Express **15**(25), 17241–17247 (2007).
27. Y.-S. No, H.-S. Ee, S.-H. Kwon, S.-K. Kim, M.-K. Seo, J.-H. Kang, Y.-H. Lee, and H.-G. Park, "Characteristics of dielectric-band modified single-cell photonic crystal lasers," Opt. Express **17**(3), 1679–1690 (2009).
28. M.-K. Seo, J.-H. Kang, M.-K. Kim, B.-H. Ahn, J.-Y. Kim, K.-Y. Jeong, H.-G. Park, and Y.-H. Lee, "Wavelength-scale photonic-crystal laser formed by electron-beam-induced nano-block deposition," Opt. Express **17**(8), 6790–6798 (2009).
29. S.-H. Kim, S.-K. Kim, and Y.-H. Lee, "Vertical beaming of wavelength-scale photonic crystal resonators," Phys. Rev. B **73**(23), 235117 (2006).
30. J.-H. Kang, M.-K. Seo, S.-K. Kim, S.-H. Kim, M.-K. Kim, H.-G. Park, K.-S. Kim, and Y.-H. Lee, "Polarized vertical beaming of an engineered hexapole mode laser," Opt. Express **17**(8), 6074–6081 (2009).
31. H.-Y. Ryu, H.-G. Park, and Y.-H. Lee, "Two-Dimensional Photonic Crystal Semiconductor Lasers: Computational Design, Fabrication, and Characterization," IEEE J. Sel. Top. Quantum Electron. **8**(4), 891–908 (2002).

1. Introduction

Ultra-small and high-quality (Q) photonic crystal (PhC) cavities [1–17] have been spotlighted for their applications in low threshold lasers [1–3], high speed modulators [4–7], single photon sources [8–10] and cavity quantum electrodynamics [11–15]. Many groups have reported various forms of ultra high-Q ($>10^6$) 2-D PhC slab cavities with small mode-volumes [16,17]. In these cavities, photons are confined in a two-dimensional fashion.

Recently the high Q/V 1-D PhC beam cavity was proposed and employed [18,19]. The compactness and the lightness of the 1-D PhC cavity have attracted researchers working on cavity-optomechanics [20,21] and compact optical-devices [22–24]. In 2008, Notomi *et al.* proposed a theoretical maximum Q-factor of $2.0\text{x}10^8$ and a modal volume of $\sim 1.4(\lambda/n)^3$ after precise tuning of the periodic ladder's size [19]. The predicted Q-factor is very high in spite of its 1-D structure.

In this work, we propose and demonstrate a new 1-D high-Q PhC beam cavity structure. The width of 1-D PhC waveguide structure is parabolically tapered in order to create a Gaussian-shaped photonic well. The formation of high-Q modes is identified near the photonic well region. The smooth parabolic perturbation minimizes scattering losses [25]. The existence of the newly-generated resonant mode is experimentally confirmed through the lasing action of 1-D PhC lasers. We also found that the vertical emission characteristics can be controlled by modifying the symmetry of the cavity structure.

#122441 - $15.00 USD Received 8 Jan 2010; revised 25 Feb 2010; accepted 1 Mar 2010; published 4 Mar 2010

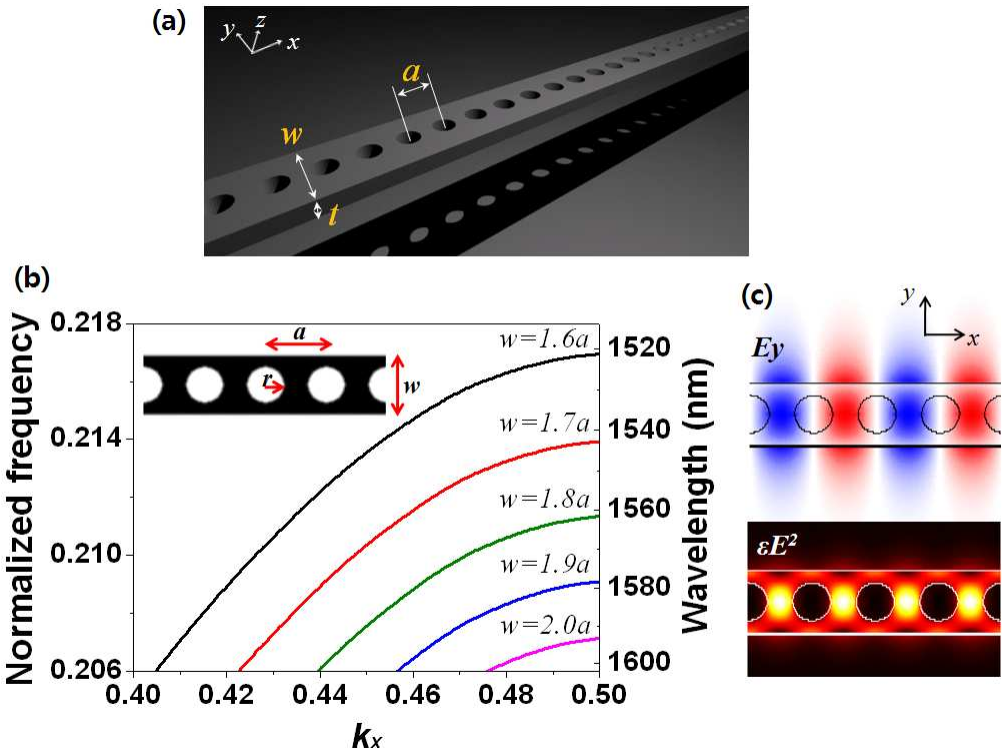

Fig. 1. (a) Schematic of 1-D periodic structure. (b) Dispersion of 1-D photonic lattices. (c) Electric field (*Ey*) distribution and electric energy distribution.

2. Design of 1-D parabolic-beam PhC cavity

Consider a 1-D periodic PhC waveguide structure where air holes are drilled along *x* direction periodically, as shown in Fig. 1(a). We choose dielectric guided modes in which electric fields are concentrated in the dielectric region. Dispersion characteristics of the dielectric guided modes are shown in Fig. 1(b), for 1-D PhC structures of different beam widths and a fixed air-hole size. Note that the normalized cutoff frequency decreases with the beam width (*w*). Getting the width thinner makes the effective refractive index of the guiding structure decrease, and thus the cutoff wavelength (frequency) becomes smaller (larger) accordingly.

#122441 - $15.00 USD Received 8 Jan 2010; revised 25 Feb 2010; accepted 1 Mar 2010; published 4 Mar 2010

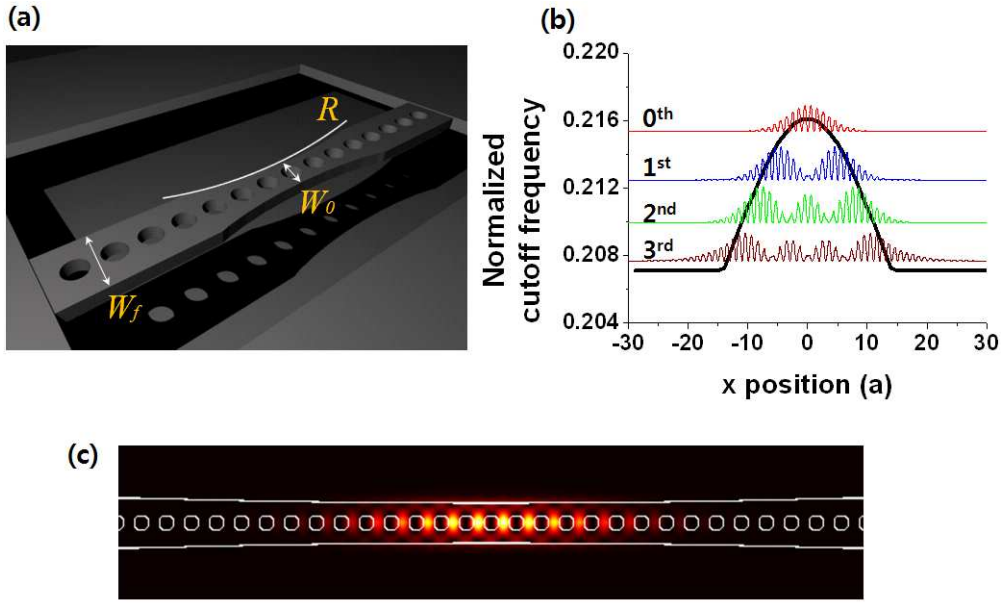

Fig. 2. (a) Schematic of 1-D parabolic-beam PhC cavity. R is a tapering radius of curvature, W_0 is the width of the thinnest central waist, and W_f is the width of the 1-D structure. (b) The black line plots the expected normalized cutoff frequency as a function of x position of the parabolic-beam. The graph also shows the resonant modes found in the photonic well. The respective resonant frequencies are 0.2153, 0.2125, 0.2099, and 0.2077. (c) Electric field intensity (E^2) distribution of the fundamental mode.

So far tuning of 1-D periodic PhC cavity was achieved by modulation air-hole size or lattice constant [19,22,24]. Here, we design a new type of cavity by tuning the width of 1-D PhC beam waveguide structure as shown in Fig. 2(a). It is well known that the parabolic shape of cutoff frequency is advantageous in obtaining high Q factors [16,26]. The width of the 1-D parabolic-beam PhC cavity is tuned parabolically as $W = W_0 + 2R - 2R\sqrt{1-(x/R)^2}$. Assuming that the cutoff frequency of the guided mode faithfully follows the dispersion characteristics predicted in Fig. 1(b), the shift of the cutoff frequency is expected to be proportional to x^2. This parabolic variation makes the Gaussian-shaped optical well in which confined photon modes can reside [26]. Figure 2(b) plots the cutoff frequency as a function of x position. Three-dimensional finite-difference time-domain (3-D FDTD) computations predict that there exist four confined modes in this photonic well. These modes originate from the dielectric band, so photon energy is mostly located in the region of dielectric as shown in Fig. 2(c). We, thus, expect the strong interactions between the dielectric gain medium and the modal field [27]. Refractive index of the material (n), slab thickness (t), hole radius (r), curvature radius of the waist (R), the width of the center (W_0) and the final width(W_f) are 3.4, 0.8a, 0.3a, 500a, 1.6a, 2.0a respectively, where a is lattice constant of periodic air holes. The normalized frequency of the fundamental mode, its Q factor and mode volume are 0.2153, ~7,000,000 and $0.83(\lambda/n)^3$, respectively.

#122441 - $15.00 USD Received 8 Jan 2010; revised 25 Feb 2010; accepted 1 Mar 2010; published 4 Mar 2010

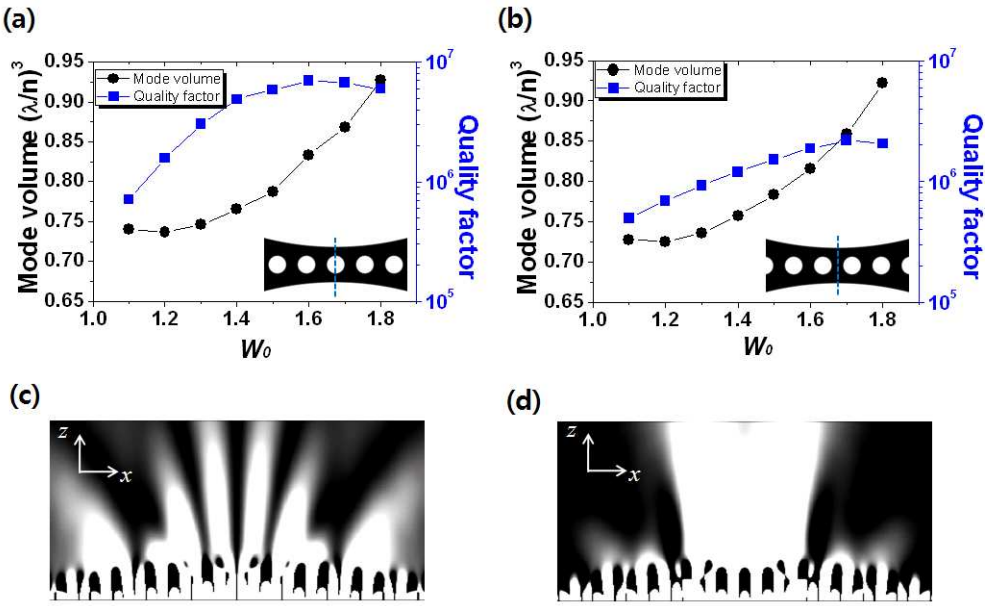

Fig. 3. Mode volumes and Q factors of (a) the air-center (b) the dielectric-center parabolic-beam cavity. Poynting vectors (S_z) of (c) the air-center (d) the dielectric-center parabolic-beam cavity (side view).

We identify two kinds of cavities of different symmetries as shown in Fig. 3 [28]. The air-center cavity [Fig. 3(a)] is symmetric with respect to the central air hole and the dielectric-center cavity [Fig. 3(b)] is symmetric with respect to the line passing through the central dielectric region. As shown in Fig. 1(c), the E_y field of the air-center cavity has an odd symmetry with a node at the symmetry plane. Therefore, the cavity loss can be effectively suppressed and the Q factor can be high [29,30]. In comparison, the dielectric-center cavity has an even symmetry with an anti-node at the center. In this case, the vertical emission loss is larger than that of the air-center cavity. These two effects are depicted in the emission profiles of Fig. 3(c) and 3(d).

3. 1. D parabolic-beam PhC laser

The 1-D parabolic-beam PhC laser structure is fabricated on a 280-nm-thick free-standing InGaAsP slab, as shown in Fig. 4(a) [30,31]. Three pairs of InGaAsP quantum wells emitting near 1.5 μm are employed as the gain medium of the laser. The lattice constant (a), the radius of the air hole (r), and the curvature radius of waist (R) of the fabricated PhC structure are ~350 nm, 100 nm, and 100 μm, respectively. The cavity is pulse-pumped by a 980-nm InGaAs laser diode (10 ns pulses, ~1% duty cycle) using a 50x microscope objective lens with a numerical aperture (N.A.) of 0.85. Threshold behavior is observed and the lasing threshold (irradiated power) is ~1.34 mW, as shown in Fig. 4(b), and the corresponding absorbed power by the slab (effective pump power) is 86 μW. We observe a single lasing peak of the fundamental mode (λ = 1487.5nm) as shown in the PL spectrum [Fig. 4(c)]. The output field is y-polarized with a measured polarization extinction ratio (PER) of 6.3:1. Considering that the resonant mode is basically a TE mode, this polarization characteristic is understandable. When the incident power increase up to 1.9 mW, two peaks of 0th mode (λ_0 = 1487.5 nm) and 1st mode (λ_1 = 1519.3 nm) are observed [Fig. 4(c)]. To confirm the modes, we compare near-field profiles of the measured CCD image and the vertical component of the Poynting vector obtained by 3-D FDTD computation. The computation is performed with the real fabricated structure, which are directly obtained from the SEM images, as input data. The calculations reflect all fabrication imperfections [2,27,28]. Figure 4(d) is the CCD image of the fundamental mode of air-center cavity [inset of Fig. 4(c)] in which the symmetry axis passes

#122441 - $15.00 USD Received 8 Jan 2010; revised 25 Feb 2010; accepted 1 Mar 2010; published 4 Mar 2010

through the center of air hole. Observe that the central node between two bright spots in Fig. 4(d) and 4(e). The calculated vertical component of the propagating Poynting vector at a vertical position of 1.0 μm above the slab matches well with the measured near-field profile of the air-center cavity. The spectral separation ($\Delta\lambda_{01}$ = 31.8 nm) between 0th mode and 1st mode agrees well with the 3-D FDTD computations ($\Delta\lambda_{01}$ = 33.6 nm).

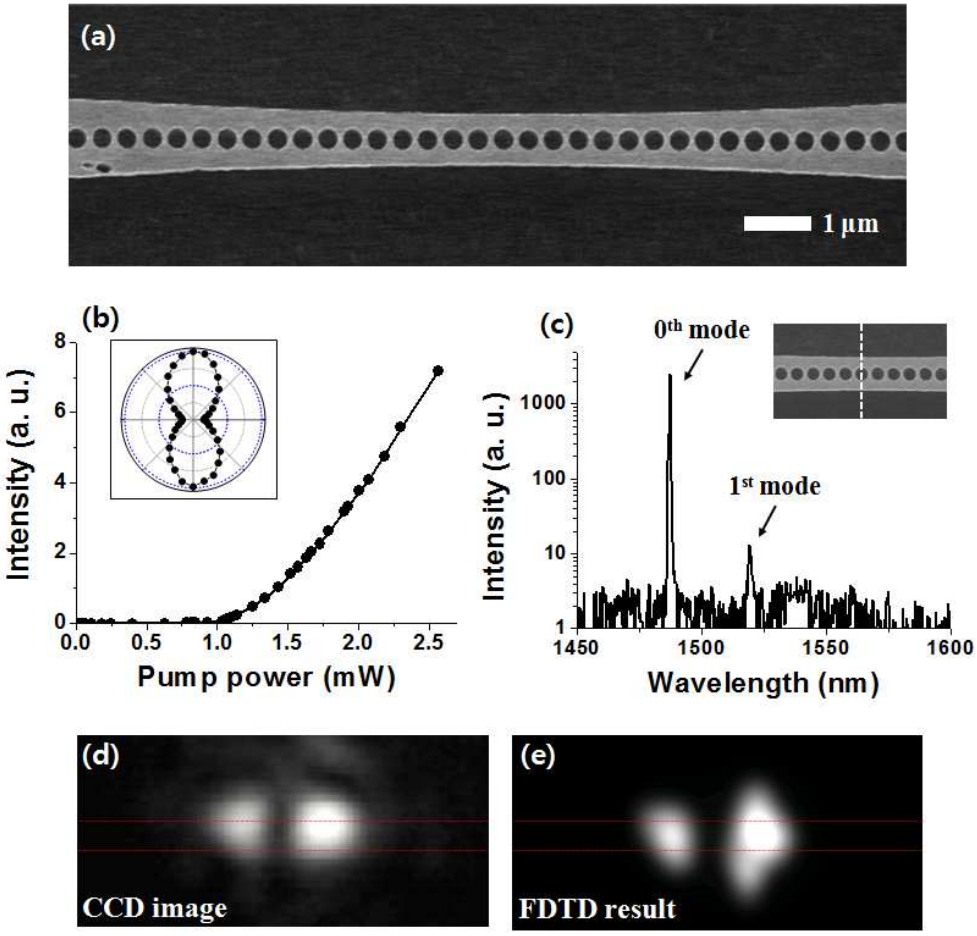

Fig. 4. (a) Scanning electron microscope (SEM) image of fabricated sample. (b) Light-in versus light-out curve and polarization characteristics of the fundamental mode of the fabricated sample. (c) Measured PL spectra and the SEM image of air-center cavity. (d) Measured IR CCD image of the fundamental mode of air-center cavity. The dotted red line indicates the boundary of the fabricated sample. (e) The vertical component of the Poynting vector obtained with the use of the structural data of the inset of (c).

The optical properties of dielectric-center cavity are measured with the same manner of air-center cavity (Fig. 5). The fundamental mode (λ_0 = 1524 nm) and the first mode (λ_1 = 1550 nm) are observed as shown in Fig. 5(a). Mode separation of the two peaks is 26 nm and the calculated value is 21 nm. The fundamental mode of the dielectric-center shows a central intensity maximum which prefers the vertical emission [Fig. 5(b)]. These emission properties agree well with the 3-D FDTD calculation of Fig. 5(c). To see only the emission of the fundamental mode, we employ the 1524 nm band-pass filter. The measured CCD image is blurred by the objective lens and the band-pass filter.

#122441 - $15.00 USD Received 8 Jan 2010; revised 25 Feb 2010; accepted 1 Mar 2010; published 4 Mar 2010

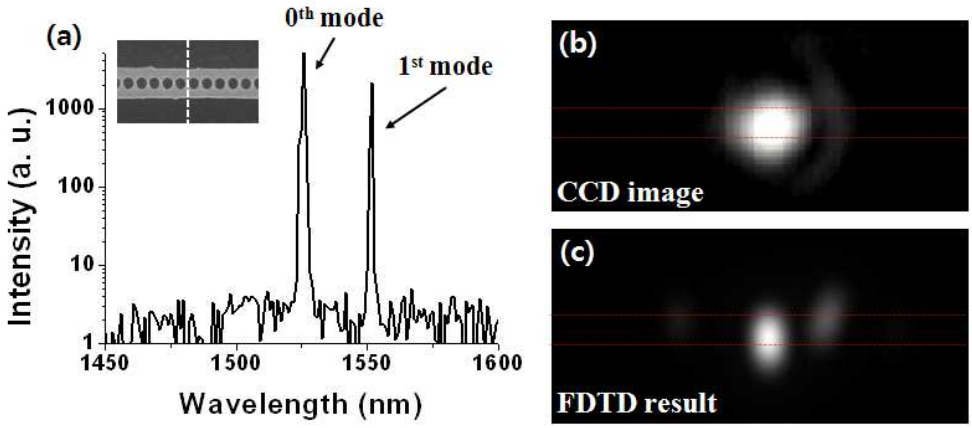

Fig. 5. (a) Measured PL spectra and the SEM image of dielectric-center cavity. (b) Measured CCD image of the 0th mode of dielectric-center cavity. (c) The calculated vertical component of the Poynting vector.

4. Summary

The new type of 1-D cavity, parabolic-beam PhC cavity, is proposed and demonstrated by the lasing behaviors. This type of laser has a small physical size compared to the conventional 2-D PhC lasers. It also has a high Q/V value. We believe that this type of 1-D parabolic-beam PhC resonator can be useful for photonic integrated circuits and cavity quantum electrodynamics.

Acknowledgments

This research was supported by WCU (World Class University) program through KOSEF (Korea Science and Engineering Foundation) funded by the Ministry of Education, Science and Technology (grant number: R31-2008-000-10071-0), by the National Research Foundation of Korea funded by the Korea government (MEST) (grant number: 2009-0093863), and by Basic Science Research Program through the National Research Foundation of Korea funded by the Ministry of Education, Science and Technology (grant number: 2009-0087691).

#122441 - $15.00 USD Received 8 Jan 2010; revised 25 Feb 2010; accepted 1 Mar 2010; published 4 Mar 2010